공학석사학위논문

제한된 데이터 조건 하에서 회전체 시스템의 고장 진단을 위한 스펙트럼 지도 적대적 생성 네트워크 기반의 신호 생성 기법

Spectrum-guided GAN: A Reliable Signal Generation Approach for Fault Diagnosis of Rotating Machinery with Limited Data

2023 년 2 월

서울대학교 대학원

기계공학부

김 태 훈

제한된 데이터 조건 하에서 회전체 시스템의 고장 진단을 위한 스펙트럼 지도 적대적 생성 네트워크 기반의 신호 생성 기법

Spectrum-guided GAN: A Reliable Signal Generation Approach for Fault Diagnosis of Rotating Machinery with Limited Data

지도교수 윤 병 동
이 논문을 공학석사 학위논문으로 제출함

2022 년 10 월

서울대학교 대학원
기계공학부
김 태 훈

김 태 훈의 공학석사 학위논문을 인준함
2022 년 12 월

위 원 장 : 김 윤 영 (인)

부위원장 : 윤 병 동 (인)

위 원 : 김 도 년 (인)

Abstract

Spectrum-guided GAN: A Reliable Signal Generation Approach for Fault Diagnosis of Rotating Machinery with Limited Data

Taehun Kim
Department of Mechanical Engineering
The Graduate School
Seoul National University

Generative adversarial network (GAN)-based data generation has been widely investigated in the field of fault diagnosis to solve a class-imbalance problem which is caused by lack of fault data in the real industry. Although much of the works have validated that GAN is effective to handle the class-imbalance problem for fault diagnosis, several critical limitations still remain. First, GAN requires sufficient amount of data for training, despite it should leverage only small amount of data to improve the classifier. Moreover, GAN trained with only small amount of time-series data tends to generate identical data that is similar process with oversampling. Second, randomness exists while sampling the latent vectors from prior distribution. Hence, inappropriately extracted latent vectors rather lower performance of a classifier. Therefore, in this paper,

we propose the spectrum-guided GAN which generates magnitude and phase spectra in frequency domain instead of producing time-series signal. In addition, a new sampling method based on density of features inside generator via principal component analysis (PCA) is introduced to replace a conventional random sampling. The proposed method is validated with GE Bently Nevada RK4 rotor kit and Signallink rotor-testbed (KAMP-Rotor) dataset. The results show that the proposed method outperforms the conventional GAN and the density-based sampling method enhances the reliability of the sampling process.

Keywords: Fault diagnosis
Rotating Machinery
Class-imbalance
Generative adversarial network (GAN)
Principal component analysis (PCA)

Student Number: 2021-20322

Table of Contents

Abstract ..... **i**

List of Tables ..... **v**

List of Figures ..... **vi**

Nomenclatures ..... **viii**

Chapter 1 Introduction **1**

1.1 Motivation 1

1.2 Dissertation Layout 5

Chapter 2 Theoretical Backgrounds **6**

2.1 Wasserstein GAN-Gradient Penalty (WGAN-GP) 6

2.2 Controllable approaches of GAN 7

2.3 Principal component analysis (PCA) 8

2.4 Kernel density estimation (KDE) 8

Chapter 3 Proposed Method **9**

3.1 Spectrum-guided GAN 9

3.2 Density-based Sampling via PCA 11

Chapter 4 Experimental Validation **13**

4.1 Case 1: Signallink Rotor-testbed (KAMP-Rotor) 13
4.1.1 Model and Data Description 13
4.1.2 Time- and Frequency-domain Representation 15
4.1.3 Comparative Study 16
4.1.4 Result of Density-based Sampling 17
4.2 Case 2: GE Bently Nevada RK4 rotor kit 18
4.2.1 Model and Data Description 18
4.2.2 Time- and Frequency-domain Representation 19
4.2.3 Comparative Study 20
4.2.4 Result of Density-based Sampling 21

Chapter 5 Conclusion 23

References 24

국문 초록 27

List of Tables

Table 4-1 Hyperparameters setting of GAN and classifier for case 1

Table 4-1 Hyperparameters setting of GAN and classifier for case 1

Table 4-1 Hyperparameters setting of GAN and classifier for case 1

Table 4-1 Hyperparameters setting of GAN and classifier for case 1

List of Figures

Figure 1-1 The effect of class-imbalanced dataset on the decision boundary.....3

Figure 1-2 The architecture of conventional GAN 4

Figure 1-3 Signals generated by inappropriate latent vectors.....4

Figure 1-1 The effect of class-imbalanced dataset on the decision boundary.....3

Figure 1-2 The architecture of conventional GAN 4

Figure 1-3 Signals generated by inappropriate latent vectors.....4

Figure 3-1 The architecture of spectrum-guided GAN 9

Figure 3-2 Flowchart of spectrum-guided GAN with density-based sampling 11

Figure 3-3 Density-based sampling and mapping to latent vectors 12

Figure 4-1 The architecture of GAN and classifier.....14

Figure 4-2 Signallink rotor-testbed (KAMP-Rotor) 15

Figure 4-3 Time- and frequency-domain representation for KAMP-Rotor.....16

Figure 4-4 Accuracy and f1-score for KAMP-Rotor under imbalance ratio of 10 17

Figure 4-5 Average probability in accordance with the threshold 18

Figure 4-6 GE Bently Nevada RK4 rotor kit 19

Figure 4-7 Time- and frequency-domain representation for RK4 rotor kit..... 20

Figure 4-8 Accuracy and f1-score for RK4 rotor kit under imbalance ratio of 10 21

Figure 4-9 Average probability in accordance with the threshold 22

Nomenclatures

GAN	Generative adversarial network
PCA	Principal component analysis
KDE	Kernel density estimation
TL	Transfer learning
DA	Domain adaptation
WGAN	Wasserstein generative adversarial network
GP	Gradient penalty
VAE	Variational autoencoder
L_{WGAN}	Loss function of WGAN
$L_{WGAN-GP}$	Loss function of WGAN-GP
x	Real data
$\hat{x}$	Generated data
P_r	Distribution of real data
P_g	Distribution of generated data
D	Discriminator of GAN
λ	Coefficient of gradient penalty
λ_{L1}	Coefficient of L1 regularization
$\hat{f}_w$	Estimated density function
N	Number of data
w	Bandwidth for density estimation
K	Kernel function
D_{loss}	Objective function of discriminator
G_{loss}	Objective function of generator
∇	Gradient operator

w_G	Weights in generator
$\hat{X}(f)$	Generated frequency spectrum
$\hat{A}$	Generated magnitude spectrum
$\hat{\theta}$	Generated phase spectrum
$\mathbf{h}_{1:20k}$	Feature tensors of a certain layer in the generator
$\hat{G}_{N-1}$	Output of (N-1)th layer of generator
$\mathbf{z}_{1:20k}$	Latent vectors
$\mathbf{h}_{1:20k}^{proj}$	Projected feature tensors to subspace
U	Matrix composed of orthonormal eigenvectors of $\mathbf{h}_{1:20k}^{proj}(\mathbf{h}_{1:20k}^{proj})^T$
V	Matrix composed of orthonormal eigenvectors of $(\mathbf{h}_{1:20k}^{proj})^T\mathbf{h}_{1:20k}^{proj}$
$\boldsymbol{\mu}_h$	Mean of feature tensors
$\hat{f}_w$	Estimated density function of $\mathbf{h}_{1:20k}^{proj}$
$\mathbf{h}_{1:N_{gen}}^{proj,allow}$	Projected feature tensors satisfying threshold from target generation size
$\mathbf{z}_{1:N_{gen}}^{allow}$	Converted latent vectors from $\mathbf{h}_{1:N_{gen}}^{proj,allow}$ using U

Chapter 1

Introduction

1.1 Motivation

Deep-learning-based fault diagnosis for rotating machinery has been wid ely investigated in light of its high performance and shown considerable pro gresses in recent years. Fault detection is one of application whose purpose is early detecting the anomaly state of the mechanical systems. Ko et al. su ggested a new dynamic threshold based on joint distribution of the residual and output of auto-encoder [1]. Furthermore, deep-learning-based fault classifi cation is also widely investigated by making the models recognize different patterns in the data for each state [2, 3]. Most of the deep-learning-based di agnosis models assume that the amount of data is fully enough for training and the data of each health state is balanced each other. However, acquiring the fault data in the real industry is challenging compared to collecting the normal data, because faulty machine should be immediately stopped to preve nt further losses. And the scarcity of fault data increases the disparity of the data size between the normal and fault states. This issue is called class-im balance. It lowers the model's performance because the decision boundary of

the classifier is biased to a majority class as illustrated in Figure. 1-1. Zha ng et al. summarized several approaches to handle the class-imbalance data-, feature-, and classifier-level [4]. And it can be roughly divided into two typ es: model-level approach and data-level approach. Model-level approach inclu des cost-sensitive learning. Transfer learning (TL) and domain adaptation (D A) are also one of candidate to solve the class-imbalance issue, because clas s-balanced testbed data can be fully utilized as a source dataset to correctly classify the class-imbalanced industrial target data [5, 6]. Lee et al. presente d class-conditional domain adaptation model which extracts not only shared f eatures of both source and target dataset, but also distinguishable features de pending on each health state [6]. However, TL and DA usually focus on ins ufficient labeled data issue rather than the class-imbalance problem. Moreove r, lots of research related to TL and DA assume the class-balance situation t o relieve the instability of training process. Cost-sensitive technique is defini ng different weights to each health state to consider the different amount of data. Geng et al. validated the usage of weighted cross-entropy as loss funct ion to relieve the effect of class-imbalance dataset [7]. In the data-level appr oaches, deep-learning-based generative models are widely investigated such a s variational autoencoder (VAE), and generative adversarial network (GAN). And much of the work showed GAN's high quality than the blurry outputs of VAE. Hence, GAN-based data generation approaches to handle the class-i mbalance problem in the fault diagnosis are devised by many researchers [8, 9].

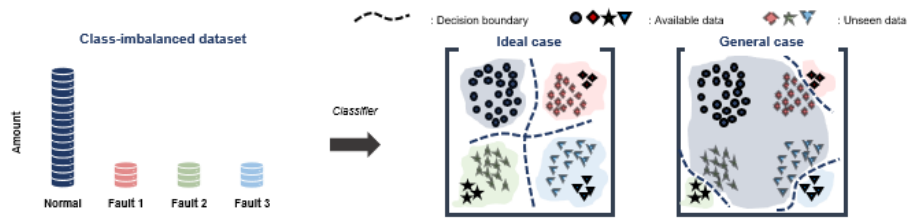

Figure 1-1 The effect of class-imbalanced dataset on the decision boundary

Though the previous research presented the availability of GAN in the field of fault diagnosis under the class-imbalance problem, several limitations still remain that should be improved. First, GAN requires another sufficient data for training the model successfully. For example, if discriminator of GAN only focuses on data distribution which is constructed by few available data, not the corresponding characteristics to each health state, then only small change of the data can confuse the discriminator due to inaccurate data distribution. In a nutshell, the discriminator distinguishes the real and fake data with a criterion whether the data belongs to the training dataset or not instead of considering the distinct properties of the data. Especially, if GAN is trained with small amount of data, the generator will try to produce the identical data with the training dataset to deceive the discriminator. The second challenge of the conventional GAN is about randomness during the sampling of latent vectors. As shown in Figure 1-2, the input of the generator is called latent vectors which are sampled from prior distribution. Though the output of the generator is only dependent on the latent vectors, controlling them is difficult because they are randomly sampled from the prior distribution. Figure 1-3 describes the examples generated by incorrectly sampled latent vectors that need to be prevented in advance.

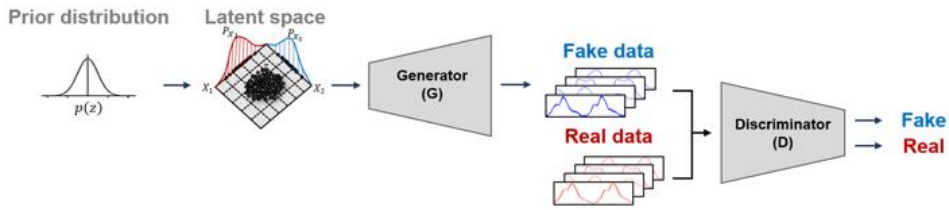

Figure 1-2 The architecture of conventional GAN

To manage these limitations, spectrum-guided GAN with a density-based new sampling method is proposed in this paper. Spectrum-guided GAN utilizes limited data for training by forcing the generator to learn the fault-related characteristics. Then, a density-based sampling method via PCA is also introduced to prevent the inappropriate latent vectors. The proposed method is validated with the two kinds of rotor-testbed: 1) GE Bently Nevada RK4 rotor rig and 2) Signallink rotor-testbed. The results show that the proposed method outperforms the conventional GAN and density-based sampling method increases the reliability of the sampling process. The main contributions of this work are summarized as follows.

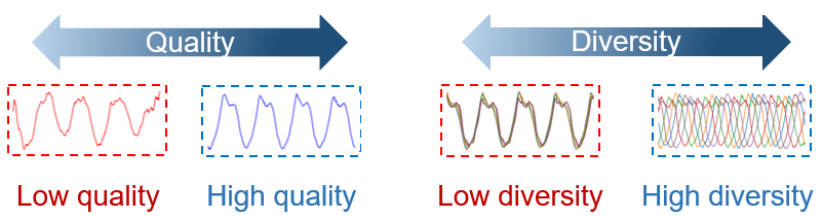

Figure 1-3 Signals generated by inappropriate latent vectors

1) A novel spectrum-guided GAN is newly proposed to alleviate the cla ss-imbalance problem by making the generator learn characteristics of each h ealth state with the help of fully utilizing the frequency spectrum, not just r aw data. And limited amount of data is utilized to validate the spectrum-gui ded GAN and reflect practical scenarios.

2) A new density-based sampling method is presented to prevent inappr opriate latent vectors. The feature tensors in a certain layer of the generator are analyzed using principal component analysis (PCA). Then, the density fu nction of the feature tensors is estimated and the sampling is processed base d on the density function. The latent vectors that are sampled from density-based sampling method is validated with pre-trained model which is trained with balanced-dataset.

1.2 Dissertation Layout

The Master's thesis is organized with five parts including this section. Chapter 2 introduces the background knowledge for the proposed method focusing on the generative adversarial network and its interpretability. Chapter 3 demonstrates the proposed spectrum-guided GAN and density-based sampling technique based on the statistical approach. Chapter 4 presents both the qualitative and quantitative results for the two case studies, and also suggests comparative results. Chapter 5 summarizes the Master's thesis and introduces future works which are related to the current research.

Chapter 2

Theoretical Backgrounds

2.1 Wasserstein GAN-Gradient Penalty (WGAN-GP)

GAN is one of the deep-learning-based generative models using adversarial learning between the generator and discriminator [10]. One of the critical challenges of conventional GAN is training stability due to the adversarial learning. Arjovsky et al. improved the stability of GAN by utilizing Wasserstein distance which is shown in Eq. (2.1). The new objective function using Wasserstein distance is written in Eq. (2.2) and it prevented gradient vanishing problem of the discriminator and enabled further training of GAN [11]. However, weights in discriminator of pre-trained Wasserstein GAN (WGAN) are gathered to the certain values due to weight clipping which is applied to WGAN to satisfy Lipschitz constraint. Therefore, Gulrajani et al. applied regularization to the gradients of the discriminator to prevent the weights distribution dispersed [12]. Due to the additional gradient penalty term as described in Eq. (2.3), WGAN-GP achieved further improvement in terms of the training stability.

$$W(\mathrm{P}_r, \mathrm{P}_g) = \sup_{\|f\|_{L\le 1}} \mathrm{E}_{x\sim \mathrm{P}_r}\left[f(x)\right] - \mathrm{E}_{\hat{x}\sim \mathrm{P}_g}\left[f(\hat{x})\right] \tag{2.1}$$

$$L_{WGAN} = \underset{\hat{x}\sim \mathrm{P}_g}{\mathrm{E}}\left[D(\hat{x})\right] - \underset{x\sim \mathrm{P}_r}{\mathrm{E}}\left[D(x)\right] \tag{2.2}$$

$$L_{WGAN-GP} = L_{WGAN} + \lambda \underset{\hat{x}\sim \mathrm{P}_g}{\mathrm{E}}\left[\left(\left\|\nabla_{\hat{x}} D(\hat{x})\right\|_2 - 1\right)^2\right] \tag{2.3}$$

2.2 Controllable approaches of GAN

Two approaches exist for analyzing the generator of GAN: Explicit and implicit approach. Explicit method is manipulating the conventional model by adding extra latent vectors to the original set of latent vectors. Chen *et al*. suggested the idea that additional categorical latent vectors can affect to the change in class. And they performed unsupervised learning which can be controlled by additional latent vectors [13]. Shoshan *et al*. also introduced additional latent vectors which are assigned to each attribute and they are separately converted through the each encoder. And they showed that the additional latent vectors can be utilized for controlling GAN [14]. On the other hand, implicit method is decomposing the generator after the training is finished. Though the outputs of the generator cannot be manipulated directly by the latent vectors, the feature tensors in each layer of the generator is arranged in the certain direction depending on the properties of the dataset. Härkönen *et al*. presented that GAN can be decomposed by applying PCA to feature tensors of the generator and achieved the latent vectors can be controlled through the method

[15].

2.3 Principal component analysis (PCA)

Dimensionality reduction method is an efficient tool to analyze high dimension. According to the manifold hypothesis, the data can be explained in much lower dimension than the original dimension [16]. PCA is one of the dimensionality reduction methods by calculating eigenvectors of covariance matrix of high dimensional features. These eigenvectors describe the principal components on which most of the data lies [17].

2.4 Kernel density estimation (KDE)

KDE is one of a non-parametric estimation method using the kernel function K to estimate the underlying distribution of a random variable x with bandwidth w. It improves the limitation of histogram which has discrete by using the kernel function. There are several kernel functions including gaussian, uniform, and Epanechnikov. Eq. (2.4) describes the KDE of random variable x and gaussian kernel function is chosen in this work for the ease of use and computation.

$$\hat{f}_w(x) = \frac{1}{Nw}\sum_{i=1}^{N} K\left(\frac{x - x_i}{w}\right) \tag{2.4}$$

Chapter 3

Proposed Method

3.1 Spectrum-guided GAN

The structure of the proposed spectrum-guided GAN is shown in Figure 3-1 Previous research about GAN in the field of fault diagnosis utilizes time-series signal with conventional objective function including Wasserstein distance which calculates the difference of feature distributions and does not consider the characteristics of the signal. Hence, the discriminator only trained with various and enough data can implicitly learn the properties of the train dataset. On the other hand, if the available dataset is not sufficient to train GAN, the discriminator cannot learn appropriate properties of the dataset, rather the generator will just copy the train dataset that is same process with oversampling. In order to avoid this problem, the spectrum-guided GAN generates frequency spectrum including magnitude and

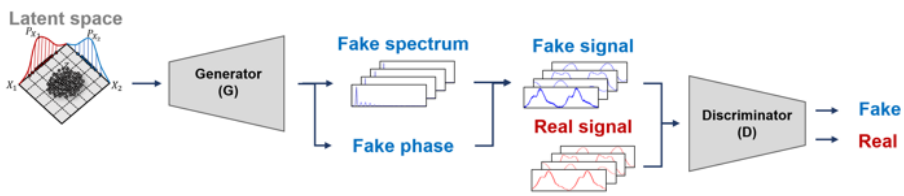

Figure 3-1 The architecture of spectrum-guided GAN

phase information to guide both the generator and discriminator to learn the characteristics of the input signal. Therefore, the proposed spectrum-guided GAN can prevent the generator from overfitting to training data.

The objective function of spectrum-guided GAN follows the conventional WGAN-GP as discussed in Chapter II-1. The only difference between loss function of generator of WGAN-GP and proposed spectrum-guided GAN is additional L1 regularization term. This term helps reduce the magnitude of frequencies which are unrelated to the target health state. The loss functions of the discriminator and the generator are shown in Eq. (3.1)-(3.2). And the fake signal should be constructed from the generated frequency spectrum using inverse Fourier transform as described in Eq. (3.3), because the generator does not generate the time-series signal and instead, it produces frequency spectrum with two channels: the first channel is assumed to the magnitude spectrum and the second channel is considered of the phase spectrum.

$$D_{loss} = \underset{\hat{x}\sim P_g}{\mathrm{E}}\left[D(\hat{x})\right] - \underset{x\sim P_r}{\mathrm{E}}\left[D(x)\right] + \lambda \underset{\hat{x}\sim P_g}{\mathrm{E}}\left[\left(\left\|\nabla_{\hat{x}} D(\hat{x})\right\|_2 - 1\right)^2\right] \tag{3.1}$$

$$G_{loss} = -\mathrm{E}\left[D(\hat{x})\right] + \lambda_{L1}\sum\left|w_G\right| \tag{3.2}$$

$$\hat{x}(n) = \frac{1}{N}\sum_{k=0}^{N-1}\hat{X}(f)\exp\left(\frac{j2\pi kn}{N}\right) \tag{3.3}$$

$$\hat{X}(f) = \hat{A}\exp\left(j\hat{\theta}\right) \tag{3.4}$$

3.2 Density-based Sampling via PCA

The concept of a new sampling method is adopted from the research of an interpretability of GAN [8]. And the flowchart of density-based sampling method is described in **오류! 참조 원본을 찾을 수 없습니다.**. Before delving into the flowchart, it is assumed that the more frequent the feature tensors are sampled, the higher the quality of the output signals are, because they will experience more updates. First, to consider almost all possible cases, 20k latent vectors are sampled from prior distribution that is chosen as normal distribution and injected to the

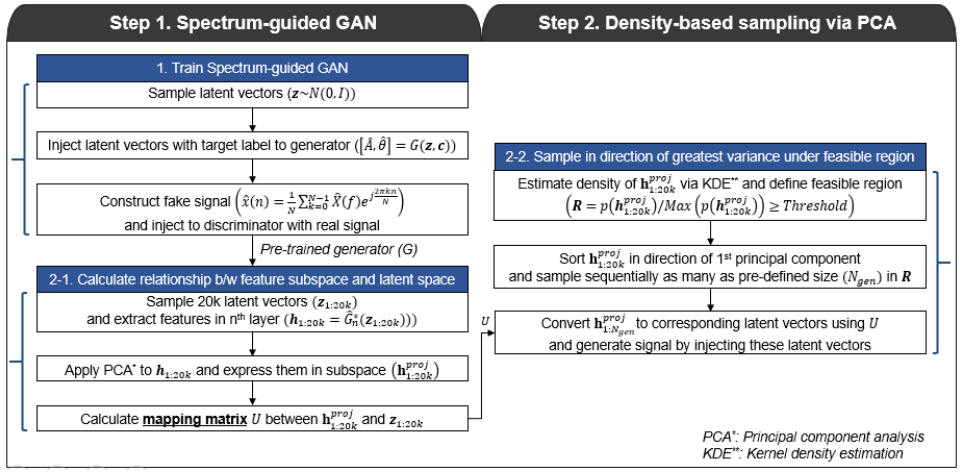

Figure 3-2 Flowchart of spectrum-guided GAN with density-based sampling

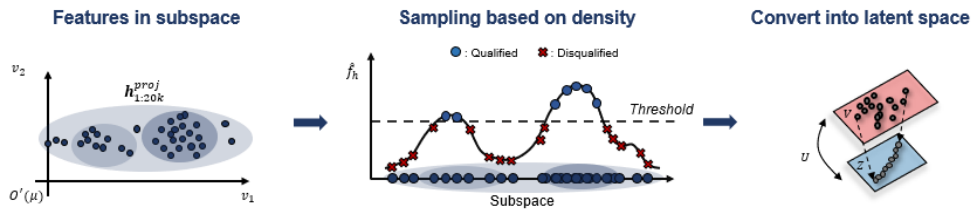

Figure 3-3 Density-based sampling and mapping to latent vectors

generator. Then, the projected feature

tensors are obtained by applying the PCA to the second to the last layer, and the mapping matrix between the projected feature tensors and the input latent vectors is calculated via least square method. The reason that the second to the last layer is chosen is that it is easier to predict which feature tensors are sampled more than the others. After arranging the projected feature tensors in the 1st principal component which has highest variance, the arranged projected feature tensors are sampled as much as the target generation size. The final latent vectors which will generate the diverse signals are obtained after multiplying the mapping matrix to the sampled feature tensors. The final latent vectors are utilized as an input of the generator.

Chapter 4

Experimental Validation

4.1 Case 1: Signallink Rotor-testbed (KAMP-Rotor)

4.1.1 Model and Data Description

The architectures of spectrum-guided GAN and classifier is constructed as illustrated in Figure 4-1. The overall architectures are same with case 2. The hyperparameters of each model is presented in Table 4-1. The KAMP-Rotor testbed is illustrated in Figure 4-2. The data type of KAMP-Rotor testbed is acceleration. The rotating speed of the test rig is 1,500 rpm (= 25 Hz) and the sampling frequency is 1,000 Hz. Therefore, the data length for each sample is set as a multiple of 40 ($=1,000/25$). In this case study, the data length is 240 which includes six wavelengths. The split ratio of train/valid/test for the classification task is 0.6, 0.2, and 0.2 each. And only the train dataset of classification task is utilized in the generation task, because completely identical dataset should be used for training the classifier and generative model. The testbed consists of 4 health states: normal, unbalance, mechanical looseness, and compound fault that is combined with unbalance and mechanical looseness. For the signal generation, only three fault states are utilized due to the abundancy of normal data in the industry. And for classification of the health states, four classes including the normal state are used.

The number of the fault state samples is fixed to 10 for both the classification and the generation task. And the number of the normal state samples is adjusted depending on the imbalance ratio in the range of 5 to 20.

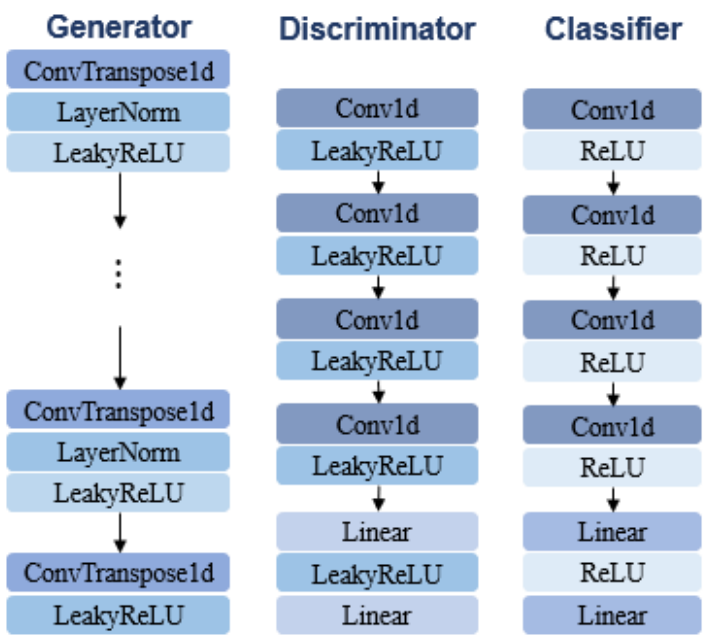

Figure 4-1 The architecture of GAN and classifier

Table 4-1 Hyperparameters setting of GAN and classifier for case 1

Task	Generation		Classification
Model	Generator	Discriminator	Classifier
Kernel	[5, 5, 5, 5, 5]	[16, 8, 4, 4]	[8, 8, 8]
Channel	[128, 128, 64, 64, 2]	[16, 64, 64, 128]	[16, 16, 16]
Dilation	[1, 2, 4, 8, 16]	/	[1, 2, 4]
Stride	/	[2, 2, 2, 1]	[2, 2, 2]
Padding	[0, 0, 1, 1, 1]	/	/
Output padding	[0, 0, 0, 0, 1]	/	/

4.1.2 Time- and Frequency-domain Representation

Time-and frequency-domain representation validate the spectrum-guided GAN in qualitative way. For the case 2 dataset, time- and frequency-domain is presented in Figure 4-3. The fundamental frequency which corresponds to rotating speed (25 Hz) is described as 1x and the harmonics of the fundamental frequency are expressed as multiples of it: 2x, 3x, 4x, …. All of the health states have components of fundamental frequency and its harmonics, though the relative magnitude of them is different each other. As illustrated in Figure 4-3, the time- and frequency-domain of generated signals correspond to those of real signals despite the proposed model is

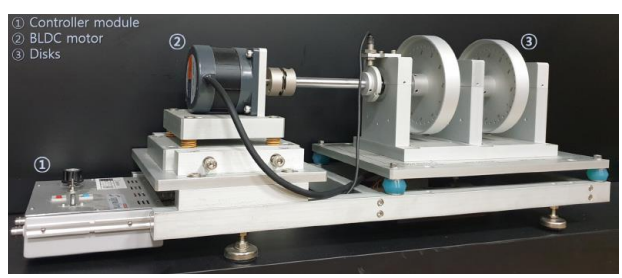

Figure 4-2 Signallink rotor-testbed (KAMP-Rotor)

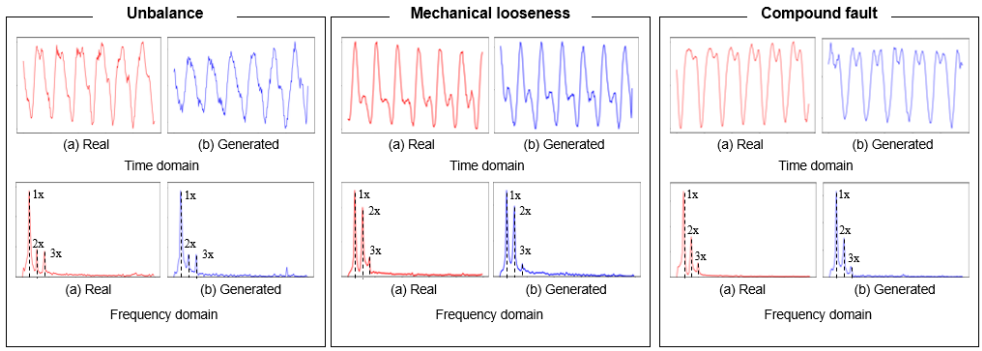

Figure 4-3 Time- and frequency-domain representation for KAMP-Rotor

trained with limited data.

4.1.3 Comparative Study

Comparative study is performed to validate the performance of the proposed model in quantitative way. For the comparative validation, three comparative models are chosen. Baseline model means the vanilla CNN model which is trained with class-imbalanced dataset. Class-weight represents the vanilla CNN model with class weighting to compensate the imbalance between the classes. And this model is also trained with class-imbalanced dataset. WGAN-GP is conventional WGAN-GP model which has same structure with the proposed method except for the hyperparameters (e.g., learning rate, kernel size, …) the number of output channels. Each trial consist of 100 epochs and the results of each model are calculated with the average of five trials. As shown in Figure 4-4 which shows the classification result with imbalance ratio 10, the accuracy of the baseline and the class-weight model is much lower with higher variances. On the other hand, WGAN-GP and proposed spectrum-guided GAN achieves about 80% accuracy. The accuracy and f1-score show similar results for

WGAN-

Table 4-2 Accuracy and f1-score for KAMP-Rotor under imbalance ratio of 10

	Baseline	**Class-weight**	**WGAN-GP**	**Proposed**
Accuracy	49.19±9.88	57.79±6.44	60.31±6.31	**66.04±5.29**
F1-score	0.42±0.11	0.56±0.064	0.57±0.059	**0.63±0.054**

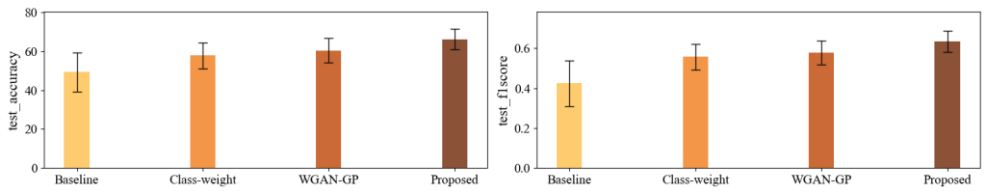

Figure 4-4 Accuracy and f1-score for KAMP-Rotor under imbalance ratio of 10

GP and proposed model in KAMP-Rotor. However, the proposed model presents higher accuracy with less variance which means less sensitive to the different weight initialization of model.

4.1.4 Result of Density-based Sampling

The results of the proposed sampling technique is presented in Figure 4-5. Each axis represents the relative density in the feature distribution and the corresponding average probability for the misalignment and the rubbing state. The average probability means that the softmax value calculated by a pre-trained CNN model which is trained with balanced dataset. Therefore, the higher the average accuracy is, the higher the quality of output signals are. In conclusion, the Figure 4-5 shows that the latent vectors sampled from the proposed sampling method can be more efficient, because the latent vectors with high quality are sampled and utilized to compensate the imbalanced dataset.

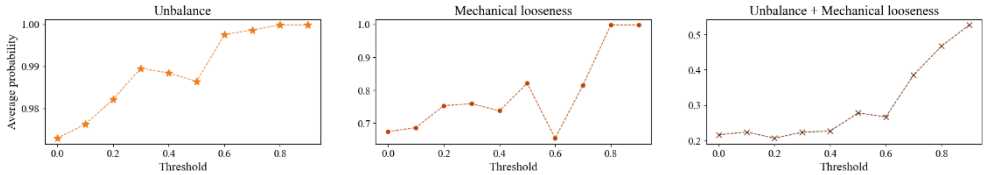

Figure 4-5 Average probability in accordance with the threshold

4.2 Case 2: GE Bently Nevada RK4 rotor kit

4.2.1 Model and Data Description

The hyperparameters for case 2 dataset are described in The RK4 rotor kit is illustrated in Figure 4-6. The data type of RK4 rotor kit is displacement. The rotating speed of the testbed is 3,600 rpm (= 60 Hz) and the sampling frequency is 8,500 Hz. Therefore, the data length for each sample is set as a multiple of 142 ($\approx 8,500/60$). The data length for each sample is set as a multiple of 142 and chosen as 568 in this case study. The split ratio of a whole dataset is same as in the case 1. The testbed consists of 5 health states: normal, misalignment, oil whirl, rubbing, unbalance. And the normal state is only used for the classification task under the class-imbalance condition and not used for the generation task. The number of the fault state samples and the normal state samples, and the imbalance ratio is same with those of case 1.

Table 4-3 Hyperparameters setting of GAN and classifier for case 2

Task	Generation		Classification
Model	Generator	Discriminator	Classifier
Kernel	[4, 4, 4, 4, 6, 6]	[16, 8, 4, 4]	[8, 8, 8]
Channel	[128, 128, 64, 64, 16, 2]	[16, 64, 64, 128]	[16, 16, 16]
Dilation	[1, 2, 4, 8, 16, 32]	/	[1, 2, 4]
Stride	/	[2, 2, 2, 1]	[2, 2, 2]
Padding	[0, 0, 0, 0, 0, 1]	/	/
Output padding	/	/	/

4.2.2 Time- and Frequency-domain Representation

For the case 1 dataset, time- and frequency-domain is presented in Figure 4-7. The fundamental frequency which corresponds to the rotating speed (60 Hz) is described as 1x and the harmonics of the fundamental frequency are expressed as multiples of it: 2x, 3x, 4x, …. Except oil whirl, all of the health states have components of fundamental frequency and its harmonics, though the relative magnitude of them is different each other. In the oil whirl's case, sub-harmonic component exists instead of the harmonics due to the oil whirl's different mechanism which is affected by lubricant in the journal bearing. The sub-harmonic frequency

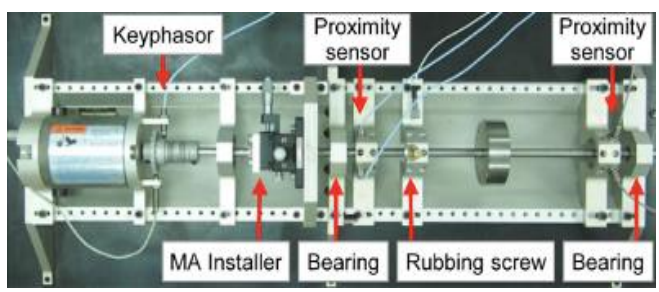

Figure 4-6 GE Bently Nevada RK4 rotor kit

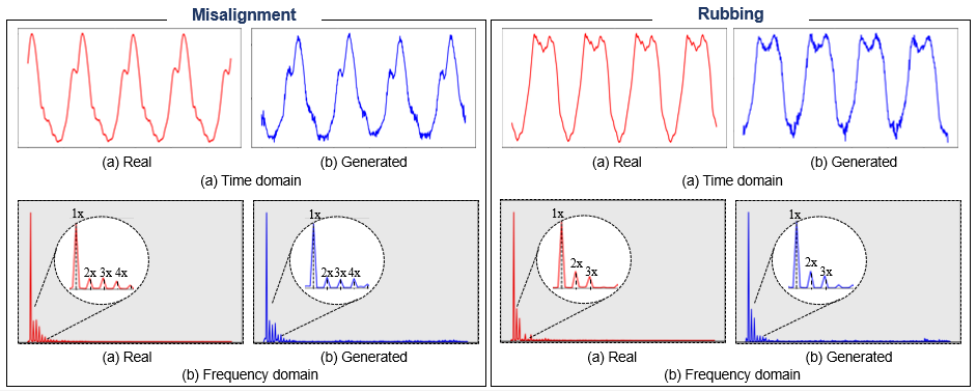

Figure 4-7 Time- and frequency-domain representation for RK4 rotor kit

is described as 0.5x. As illustrated in Figure 4-7, the time- and frequency-domain of generated signals correspond to those of real signals despite the proposed model is trained with limited data.

4.2.3 Comparative Study

For the comparative validation, the same three comparative models are utilized: baseline, class-weight, and WGAN-GP. Figure 4-8 presents the classification result with imbalance ratio 10. The result of the proposed model shows considerable discrepancy compared with the comparative models.

Table 4-4 Accuracy and f1-score for RK4 rotor kit under imbalance ratio of 10

	Baseline	**Class-weight**	**WGAN-GP**	**Proposed**
Accuracy	49.19±9.88	57.79±6.44	60.31±6.31	**66.04±5.29**
F1-score	0.42±0.11	0.56±0.064	0.57±0.059	**0.63±0.054**

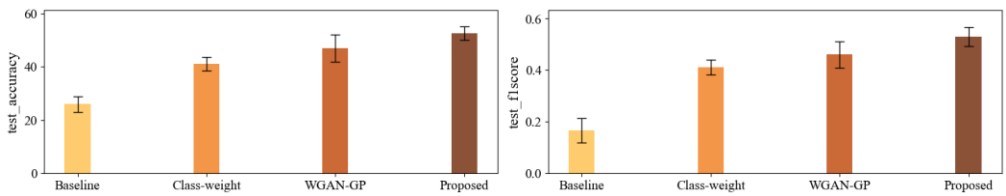

Figure 4-8 Accuracy and f1-score for RK4 rotor kit under imbalance ratio of 10

4.2.4 Result of Density-based Sampling

The results of the proposed sampling technique is presented in Figure 4-9. Each axis represents the relative density in the feature distribution and the corresponding average probability for the misalignment and the rubbing state. The average probability means that the softmax value calculated by a pre-trained CNN model which is trained with balanced dataset. Therefore, the higher the average accuracy is, the higher the quality of output signals are. In conclusion, the Figure 4-9. shows that the latent vectors sampled from the proposed sampling method can be more efficient, because the latent vectors with high quality are sampled and utilized to compensate the imbalanced dataset.

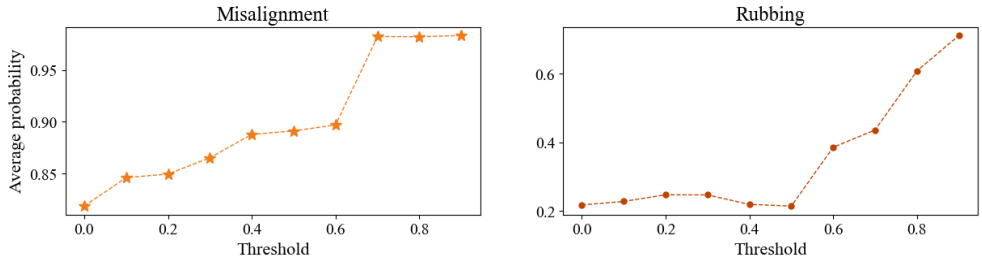

Figure 4-9 Average probability in accordance with the threshold

Chapter 5

Conclusion

In this paper, a new signal generation approach is proposed under the limited data available through the spectrum-guided GAN and the density-based sampling method. The proposed method is validated with two rotor-testbeds: Signallink rotor-testbed and GE Bently Nevada RK4 rotor kit. The results even outperformed the conventional WGAN-GP for both cases. It is expected to be utilized and developed in the filed of the fault diagnosis for various kinds of rotating machinery with few amounts of data available. Furthermore, distinguishing the quality of the generated signals is proposed via density-based sampling method. For future works, the generative model for non-stationary signals will be investigated and a new quantitative metric for evaluating the quality of signals also will be explored to enhance the density-based sampling method by defining appropriate threshold.

References

[1] J. U. Ko, K. Na, J.-S. Oh, J. Kim, and B. D. Youn, "A new auto-encoder-based dynamic threshold to reduce false alarm rate for anomaly detection of steam turbines," *Expert Systems with Applications,* vol. 189, p. 116094, 2022.

[2] Z. Chen, K. Gryllias, and W. Li, "Intelligent fault diagnosis for rotary machinery using transferable convolutional neural network," *IEEE Transactions on Industrial Informatics,* vol. 16, no. 1, pp. 339-349, 2019.

[3] H. Shao, M. Xia, G. Han, Y. Zhang, and J. Wan, "Intelligent fault diagnosis of rotor-bearing system under varying working conditions with modified transfer convolutional neural network and thermal images," *IEEE Transactions on Industrial Informatics,* vol. 17, no. 5, pp. 3488-3496, 2020.

[4] T. Zhang *et al.*, "Intelligent fault diagnosis of machines with small & imbalanced data: A state-of-the-art review and possible extensions," *ISA transactions,* vol. 119, pp. 152-171, 2022.

[5] S. Al-Stouhi and C. K. Reddy, "Transfer learning for class imbalance problems with inadequate data," *Knowledge and information systems,* vol. 48, pp. 201-228, 2016.

[6] J. Lee, M. Kim, J. U. Ko, J. H. Jung, K. H. Sun, and B. D. Youn, "Asymmetric inter-intra domain alignments (AIIDA) method for intelligent fault diagnosis of rotating machinery," *Reliability Engineering & System Safety,* vol. 218, p. 108186, 2022.

[7] Y. Geng, Z. Wang, L. Jia, Y. Qin, and X. Chen, "Bogie fault diagnosis under variable operating conditions based on fast kurtogram and deep residual learning towards imbalanced data," *Measurement,* vol. 166, p. 108191, 2020.

[8] S. Liu, H. Jiang, Z. Wu, and X. Li, "Data synthesis using deep feature enhanced generative adversarial networks for rolling bearing imbalanced fault diagnosis," *Mechanical Systems and Signal Processing,* vol. 163, p. 108139, 2022.

[9] M. Zareapoor, P. Shamsolmoali, and J. Yang, "Oversampling adversarial network for class-imbalanced fault diagnosis," *Mechanical Systems and Signal Processing,* vol. 149, p. 107175, 2021.

[10] I. J. Goodfellow *et al.*, "Generative adversarial networks (2014)," *arXiv preprint arXiv:1406.2661,* vol. 1406, 2014.

[11] M. Arjovsky, S. Chintala, and L. Bottou, "Wasserstein generative adversarial networks," in *International conference on machine learning*, 2017: PMLR, pp. 214-223.

[12] I. Gulrajani, F. Ahmed, M. Arjovsky, V. Dumoulin, and A. C. Courville, "Improved training of wasserstein gans," *Advances in neural information processing systems,* vol. 30, 2017.

[13] X. Chen, Y. Duan, R. Houthooft, J. Schulman, I. Sutskever, and P. Abbeel, "Infogan: Interpretable representation learning by information maximizing generative adversarial nets," *Advances in neural information processing systems,* vol. 29, 2016.

[14] A. Shoshan, N. Bhonker, I. Kviatkovsky, and G. Medioni, "Gan-control: Explicitly controllable gans," in *Proceedings of the IEEE/CVF international conference on computer vision*, 2021, pp. 14083-14093.

[15] E. Härkönen, A. Hertzmann, J. Lehtinen, and S. Paris, "Ganspace: Discovering interpretable gan controls," *Advances in Neural Information Processing Systems,* vol. 33, pp. 9841-9850, 2020.

[16] T. Lin and H. Zha, "Riemannian manifold learning," *IEEE transactions on pattern analysis and machine intelligence,* vol. 30, no. 5, pp. 796-809, 2008.

[17] K. Pearson, "LIII. On lines and planes of closest fit to systems of points in space," *The London, Edinburgh, and Dublin philosophical magazine and journal of science,* vol. 2, no. 11, pp. 559-572, 1901.

[18] 중소벤처기업부, Korea AI Manufacturing Platform(KAMP), 회전기계 고장유형 AI 데이터셋, KAIST(기계공학과 이필승 교수), 2021.12.27., https://kamp-ai.kr

국문 초록

제한된 데이터 조건 하에서 회전체 시스템의 고장 진단을 위한 스펙트럼 지도 적대적 생성 네트워크 기반의 신호 생성 기법

서울대학교 대학원

기계공학부

김 태 훈

실 산업에서 고장 신호 데이터 부족으로 발생하는 클래스 불균형을 해결하기 위해 적대적 생성 네트워크 기반의 신호 생성 연구가 활발히 주목받고 있다. 클래스 불균형 상황에서 고장 진단을 해결하기 위해 다수의 논문에서 적대적 생성 네트워크가 효과적임을 입증했음에도 불구하고, 몇 가지 치명적인 한계들이 존재한다. 첫 번째로, 클래스 불균형 조건의 고장 진단에서 적대적 생성 네트워크가 분류 모델의 성능을 개선할 수 있으나, 적대적 생성 모델을 학습하기 위한 데이터가 충분히 많이 필요하다는 문제점이 존재한다. 게다가 적은 양의 데이터로 학습된 적대적 생성 네트워크는 오버샘플링과 같이 학습 데이터와 동일한 데이터를 생성하는, 모드 붕괴 현상을 야기할 수 있다. 두

번째로, 신호를 생성하기 위한 적대적 생성 네트워크의 잠재 벡터 샘플링 과정에서 무작위성이 존재한다. 일반적인 적대적 생성 네트워크의 샘플링은 사전 분포로부터 무작위로 추출하기에, 부적절한 잠재 벡터로부터 생성된 신호들이 오히려 분류 모델의 성능을 악화시킬 수 있다. 따라서, 본 학위논문에서는 (1) 적은 데이터로 다양한 신호를 생성하기 위해 신호의 특성인 주파수 스펙트럼을 활용한 스펙트럼 지도 적대적 생성 네트워크를 제안하며, (2) 기존 샘플링 방식의 무작위성으로 인한 부적절한 신호 생성을 방지하기 위해 주성분 분석 기반 고차원 특성 공간의 매니폴드 분석으로 새로운 샘플링 기법을 제안한다.

주요어: 고장 진단
회전체
클래스 불균형
적대적 생성 네트워크
주성분 분석

학 번: 2021-20322